Rev. Roum. Sci. Techn.– Électrotechn. et Énerg.
Vol. **66**, *3*, pp. 169–174, Bucarest, 2021

CONTROL OF PARALLEL MULTICELLULAR DC/AC CONVERTER INCLUDING MONOLITHIC INTER-CELL TRANSFORMER IN A REAL-TIME ENVIRONMENT

SALAH HANAFI [1], MOHAMMED KARIM FELLAH[1], YOUCEF DJERIRI[1], MOHAMMED-FOUAD BENKHORIS[2]

Key words: Parallel multicellular converter (PMC), Inter-cell transformers (ICTs), Real-time, RT-LAB.

In this paper, we study the parallel multicellular dc/ac converter, including monolithic inter-cell transformer (ICT). This structure is very interesting when the ICT is used to ensure the magnetic coupling between the liaison inductances to eliminate the inductances currents ripple. But, if the inductances currents are not equilibrated; the magnetic circuit of the ICT will be saturated, and it causes the dysfunction of the converter. For that, we propose the sliding mode control to regulate the inductances currents. To validate this technique, a real-time simulation is made in using RT-LAB package under MATLAB/SIMULINK of a 7 cells parallel multicellular DC/AC converter including monolithic ICT controlled with sliding mode control.

1. INTRODUCTION

One of the main goals in power electronics is the increase of power density in converters. In recent years, multilevel converters for high current power and medium voltage applications have been introduced [1].

Among these multilevel converters, the parallel multicellular converter is a very interesting topology. This structure is obtained by the parallel connection of the switching cells through liaison inductances. The connection in parallel allows dividing current constraints on switching cells in an equal manner. Also, it leads to increase the apparent frequency of the output and input current ripple [2]. As a consequence, the filters associated with the converter can be reduced and the dynamic performance increased [3]. The converter output current is equal to P times the input current, P is the number of switching cells [4].

But, the massive parallelization of commutation cells using regular inductors to connect them is not recommended due to the increase of the current ripple in each cell. To solve this problem, inter-cell transformers (ICTs) may be used since the currents of all the cells are magnetically coupled, reducing its amplitude and increasing its frequency [2]. The addition of inter-cell transformers will make the converter very sensible to the imbalance of inductances currents, which increases the risk of the saturation of the magnetic circuit and consequently the converter stopping. For that, a very efficient regulation must be used.

Several investigations on the magnetic coupling of the liaison inductances have been carried out like [1–6]. On the other hand, just a few works treat the regulation of inductances currents.

In this article, we present the sliding mode control as a technique to regulate the inductances currents of a parallel multicell dc/ac converter including monolithic inter-cell transformer. This control technique presents a fast response and a very good robustness when load parameters change. The studied system is simulated in a real-time environment with RT-LAB simulator.

Real-time simulation is an essential step in designing systems. The importance of this phase can be illustrated in asking two questions [7]:

What is the interest in using real-time simulation?

a) Time saving
   - Test engineers saved time in the testing process;
   - Problems are detected at an earlier stage in the design process;
   - The design of a device is started while the actual system is not physically available.

b) Cost reduction
   - Cost on testing a new device under real conditions will be reduced considerably;
   - Many possible configurations could be tested in a real-time system without physical modification;
   - The total cost is reduced over the entire project and system life cycle.

c) Test functionalities increased
   - In real life in a secure and simulated environment, fake and test are all possible scenarios that could happen;
   - Being able to modify all parameters and signals of the test system at a glance give as a high flexibility;
   - Test script automation in order to run tests 24 h a day, 7 days a week.

A real-time simulation what does it mean?

Using fixed-step solvers in simulation allow to solve the studied model at regular time intervals from the beginning to the end of the simulation. The interval size is known as the step size: T_s. Generally, decreasing T_s increases the accuracy of the results while increasing the time required simulating the system [8].

2. PARALLEL MULTICELLULAR CONVERTER INCLUDING MONOLITHIC ICT

Figure 1 shows a parallel multicellular converter with magnetically coupled inductances, in using monolithic inter-cell transformer.

[1] ICEPS Laboratory (Intelligent Control & Electrical Power Systems), Djillali Liabes University of Sidi Bel-Abbes. Sidi Bel-Abbes, Algeria, E-mail: sal_hanafi@outlook.com
[2] IREENA Laboratory (Institut de Recherche en Electronique et Electrotechnique de Nantes Atlantique), University of Nantes at Saint Nazaire, France

$$\begin{cases} \frac{\mathrm{d}}{\mathrm{d}t} I_{L_1} = \frac{1}{L_1}\left(- R_{L_1} I_{L_1} + S_1 . \frac{E}{2} - V_o - M \frac{\mathrm{d}}{\mathrm{d}t} I_{L_2} - M \frac{\mathrm{d}}{\mathrm{d}t} I_{L_3} - \cdots - M \frac{\mathrm{d}}{\mathrm{d}t} I_{L_P} \right), \\ \frac{\mathrm{d}}{\mathrm{d}t} I_{L_2} = \frac{1}{L_2}\left(- R_{L_2} I_{L_2} + S_2 . \frac{E}{2} - V_o - M \frac{\mathrm{d}}{\mathrm{d}t} I_{L_1} - M \frac{\mathrm{d}}{\mathrm{d}t} I_{L_3} - \cdots - M \frac{\mathrm{d}}{\mathrm{d}t} I_{L_P} \right), \\ \vdots \\ \frac{\mathrm{d}}{\mathrm{d}t} I_{L_P} = \frac{1}{L_P}\left(- R_{L_P} I_{L_P} + S_P . \frac{E}{2} - V_o - M \frac{\mathrm{d}}{\mathrm{d}t} I_{L_1} - M \frac{\mathrm{d}}{\mathrm{d}t} I_{L_2} - \cdots - M \frac{\mathrm{d}}{\mathrm{d}t} I_{L_{P-1}} \right), \\ \frac{\mathrm{d}}{\mathrm{d}t} I_L = \frac{1}{L_L}\left(V_o - \left(I_{L_1} + I_{L_2} + \cdots + I_{L_{P-1}} + I_{L_P} \right) R_L \right), \end{cases} \tag{1}$$

$$f(x) = \begin{pmatrix} -\frac{R_{L_1}}{L_1} & -\frac{M}{L_1} & \cdots & -\frac{M}{L_1} & -\frac{V_o}{L_1 \cdot I_{L_1}} \\ -\frac{M}{L_2} & -\frac{R_{L_2}}{L_2} & \cdots & -\frac{M}{L_2} & -\frac{V_o}{L_2 \cdot I_{L_2}} \\ \vdots & \vdots & \ddots & \vdots & \vdots \\ -\frac{M}{L_P} & -\frac{M}{L_P} & \cdots & -\frac{M}{L_P} & -\frac{V_o}{L_P \cdot I_{L_P}} \\ -\frac{(R_L + S_1)}{L_L} & -\frac{(R_L + S_2)}{L_L} & \cdots & -\frac{(R_L + S_P)}{L_L} & \frac{V_o}{L_L \cdot I_L} \end{pmatrix} \cdot \begin{pmatrix} I_{L_1} \\ I_{L_2} \\ \vdots \\ I_{L_P} \\ I_L \end{pmatrix}.$$

This converter is constituted by the parallel connection of P switching cells. These P cells are interconnected between them with a monolithic inter-cell transformer.

The monolithic inter-cells transformer is realized in placing together all the windings of each phase on the same magnetic core [5].

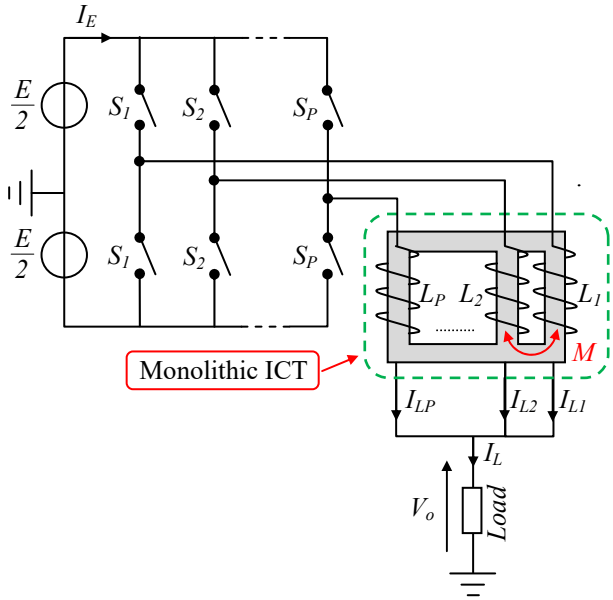

Fig. 1 – A parallel multicellular converter P cells using monolithic ICT powering an R-L load.

To find the model of the instantaneous values of the P cells parallel multicellular converter, using monolithic ICT we consider:

- The switches are ideal (saturation voltage, leakage current, downtime and null switching time).
- The switches of the same commutation cell operate in complementary.
- The magnetic coupling (mutual inductance M) is similar between the different coils.
- The supply voltage E is constant.

The equation system (1) represents the instantaneous model of a P cells dc/ac parallel multicellular arm using a monolithic inter-cells transformer with a ladder structure for the magnetic coupling of inductors and powering an R-L load.

Under assuming linear steady state behaviour, the derivative of the current through the connecting inductances dI/dt can be resumed to I as explained in [9, 10].

The equation system (1) allows us to define the state equation of this system, by taking into account the new assumption quoted above:

$$\dot{x} = f(x) + g(x) \cdot u \ , \tag{2}$$

with

$$\dot{x} = \left(\dot{I}_{L_1} \quad \dot{I}_{L_2} \quad \cdots \quad \dot{I}_{L_P} \quad \dot{I}_L \right)^{\mathrm{T}},$$

$$u = \left(S_1 \quad S_2 \quad \cdots \quad S_P \quad 0 \right)^{\mathrm{T}},$$

$$g(x) = \begin{pmatrix} \frac{E_1}{L_1} & 0 & \cdots & 0 & 0 \\ 0 & \frac{E_1}{L_2} & \cdots & 0 & 0 \\ \vdots & \vdots & \ddots & \vdots & \vdots \\ 0 & 0 & \cdots & \frac{E_1}{L_P} & 0 \\ \frac{I_{L_1}}{L_L} & \frac{I_{L_2}}{L_L} & \cdots & \frac{I_{L_P}}{L_L} & 0 \end{pmatrix},$$

where $E_1 = E/2$.

3. SLIDING MODE CONTROL

The theory of control by sliding modes was born 50 years ago after Uktin's works [11, 12]. The sliding mode control is widely used for the control of nonlinear dynamic systems such as the static converters. This technique ensures that the controlled system moves along a well-defined trajectory around an equilibrium point. We can say that the controlled system slides on a sliding surface.

The design of this control technique can be carried out in three main steps which are very dependent on each other:

1 – The choice of the sliding surface.

2 – The establishment of the conditions of the convergence existence.

3 – The determination of the control law.

Let's apply this control technique to the parallel multicellular converter using a monolithic inter-cells transformer with a ladder structure.

According to the equation (2), the state representation of the parallel multicellular converter using a monolithic inter-cells transformer with a ladder structure is given by:

$$\dot{x} = f(x) + g(x)u \ . \tag{3}$$

The sliding surface is defined by:

$$s(x) = \Delta x = x - x_{ref} \, . \tag{4}$$

The error state vector is given as follows:

$$\Delta x = \begin{pmatrix} x_1 - x_{1\,ref} \\ x_2 - x_{1\,ref} \\ \vdots \\ x_P - x_{P\,ref} \end{pmatrix} . \tag{5}$$

To check the convergence condition, we introduce the equation (6) as a Lyapunov function:

$$V = \frac{1}{2}|s(x)|^2 \ . \tag{6}$$

$$\dot{V} = s(x)\dot{s}(x) \ . \tag{7}$$

The sliding surface derivative is represented by (8):

$$\dot{s} = \dot{\Delta x} = \dot{x} - \dot{x}_{ref} \, . \tag{8}$$

In substituting (3) in (8) , we obtain:

$$\dot{s} = f(x) + g(x)u - \dot{x}_{ref} \ . \tag{9}$$

The sliding mode control structure is constituted of two parts. The continuous part u_{eq} (equivalent control) will reduce as much as we want the amplitude of the discontinuous part and thus ensure the exact linearization of the system. The discontinuous part u_n (discontinuous control) is used to check the conditions of attractiveness in the presence of a disturbance and thus ensure the system stability. These two controls equivalent and discontinuous will be synthesized in what follows.

The equivalent command is chosen in such a way that the system slides on the switching surface (the sliding surface derivative is null.):

$$u_{eq} = -(g(x))^{-1}\left(f(x) - \dot{x}_{ref} \right) . \tag{10}$$

After summation of the two commands (equivalent u_{eq} and discontinuous u_n) , we obtain the total control u (equation (11)):

$$u = u_{eq} + u_n \ . \tag{11}$$

In substituting (10) and (11) in (9) , we obtain:

$$\dot{s} = g(x)u_n \ . \tag{12}$$

To simplify the passive elements, we will introduce the matrix Q which is the passive elements matrix:

$$\dot{s} = Qg(x)u_n \ . \tag{13}$$

The Q matrix is dimensioned in such a way that the passive elements of the system to be controlled are eliminated from the control laws. For this reason, we say that the sliding mode control is robust. The matrix Q is given as follows:

$$Q = \begin{pmatrix} L_1 & 0 & \cdots & 0 & 0 \\ 0 & L_2 & \cdots & 0 & 0 \\ \vdots & \vdots & \ddots & \vdots & \vdots \\ 0 & 0 & \cdots & L_P & 0 \\ L_L & L_L & \cdots & L_L & L_L \end{pmatrix} .$$

These matrices allow us to find the Lyapunov function derivative:

$$s(x)\,\dot{s}(x) = s(x)\,Q\,g(x)\,u_n \, , \tag{14}$$

where:

$$u_n = \begin{pmatrix} u_{n1} & u_{n2} & \cdots & u_{nP} & 0 \end{pmatrix}^{\mathrm{T}} ,$$

$$s(x) = \begin{pmatrix} I_{L_1} - I_{L_1\,ref} \\ I_{L_2} - I_{L_2\,ref} \\ \vdots \\ I_{L_P} - I_{L_P\,ref} \end{pmatrix} .$$

The matrix $g(x)$ is equal to:

$$g(x) = \begin{pmatrix} \dfrac{E_1}{L_1} & 0 & \cdots & 0 & 0 \\ 0 & \dfrac{E_1}{L_2} & \cdots & 0 & 0 \\ \vdots & \vdots & \ddots & \vdots & \vdots \\ 0 & 0 & \cdots & \dfrac{E_1}{L_P} & 0 \\ \dfrac{I_{L_1}}{L_L} & \dfrac{I_{L_2}}{L_L} & \cdots & \dfrac{I_{L_P}}{L_L} & 0 \end{pmatrix} .$$

In using the Hadamard matrix product between the matrices Q and $g(x)$, the result will be equal to:

$$Qg(x)=\begin{pmatrix} E_1 & 0 & \cdots & 0 & 0 \\ 0 & E_1 & \cdots & 0 & 0 \\ \vdots & \vdots & \ddots & \vdots & \vdots \\ 0 & 0 & \cdots & E_1 & 0 \\ I_{L_1} & I_{L_2} & \cdots & I_{L_P} & 0 \end{pmatrix},$$

with:

$$\begin{aligned} Qg_1(x)&=\begin{pmatrix} E_1 & 0 & \cdots & 0 & I_{L_1} \end{pmatrix}^{\mathrm{T}}, \\ Qg_2(x)&=\begin{pmatrix} 0 & E_1 & \cdots & 0 & I_{L_2} \end{pmatrix}^{\mathrm{T}}, \\ &\vdots \\ Qg_P(x)&=\begin{pmatrix} 0 & 0 & \cdots & E_1 & I_{L_P} \end{pmatrix}^{\mathrm{T}}. \end{aligned}$$

For the state representation of the parallel multicellular converter including a monolithic ICT with ladder structure, we have:

$$\dot{s}(x)s(x)=s(x)\begin{bmatrix} Qg_1(x)u_{n1}+Qg_2(x)u_{n2} \\ +\cdots+Qg_P(x)u_{nP} \end{bmatrix}. \quad (15)$$

After calculation, we obtain:

$$\dot{s}(x)s(x)=s(x)\begin{bmatrix} (E_1+I_{L_1})u_{n1}+(E_1+I_{L_2})u_{n2} \\ +\cdots+(E_1+I_{L_P})u_{nP} \end{bmatrix}. \quad (16)$$

According to Lyapunov theorem, the stability is assured if and only if $\dot{V}(x)<0$, which brings us to write:

$$\begin{aligned} u_{n1}&=\mathrm{signs}\left[-s(x_P)(E_1+I_{L_1})\right], \\ u_{n2}&=\mathrm{signs}\left[-s(x_2)(E_1+I_{L_2})\right], \\ &\vdots \\ u_{nP}&=\mathrm{signs}\left[-s(x_P)(E_1+I_{L_P})\right], \end{aligned} \quad (17)$$

with:

$$\begin{aligned} s(x_1)&=\left(I_{L_1}-I_{L_{1\,ref}}\right), \\ s(x_2)&=\left(I_{L_2}-I_{L_{2\,ref}}\right), \\ &\vdots \\ s(x_P)&=\left(I_{L_P}-I_{L_{P\,ref}}\right). \end{aligned}$$

After calculations, we obtain the control signals matrix u:

$$\begin{aligned} S_1&=\mathrm{signs}\left(\frac{E}{2}\left(I_{L_1\,ref}-I_{L_1}\right)+I_{L_1}\left(I_{L_1\,ref}-I_{L_1}\right)\right), \\ S_2&=\mathrm{signs}\left(\frac{E}{2}\left(I_{L_2\,ref}-I_{L_2}\right)+I_{L_2}\left(I_{L_2\,ref}-I_{L_2}\right)\right), \\ &\vdots \\ S_P&=\mathrm{signs}\left(\frac{E}{2}\left(I_{L_P\,ref}-I_{L_P}\right)+I_{L_P}\left(I_{L_P\,ref}-I_{L_P}\right)\right). \end{aligned} \quad (18)$$

We will insert, now, the P commutation laws in P feedback loops (Fig. 2). A regulation loop is dedicated to each one of the state variables. This will allow us to calculate the errors compared to the reference quantities. The next step is to calculate the P switching functions in combining linearly the errors of state variables. It will only remain to introduce P hysteresis comparators to generate the P control orders of the parallel multicellular inverter P cells.

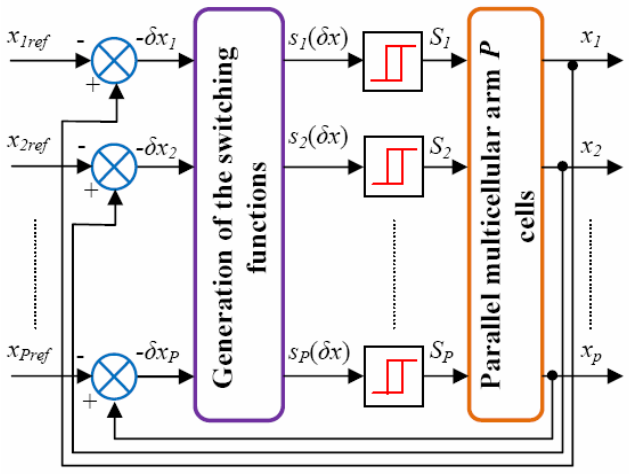

Fig. 2 – Sliding mode control technique applied to the P cells parallel multicellular converter.

4. STUDIED SYSTEM AND REAL-TIME SIMULATION RESULTS

RT-Lab [13] uses MATLAB/SIMULINK as a front-end interface for editing graphic models in block-diagram format, which are afterwards used by this real-time simulator to generate the necessary C-code for real-time simulations on a single or more target processors running Quick unix (QNX) [14].

The digital Real-Time simulation of the 7 cells parallel multicellular converter, including a monolithic ICT with ladder structure powering an R–L load is shown in Fig. 3.

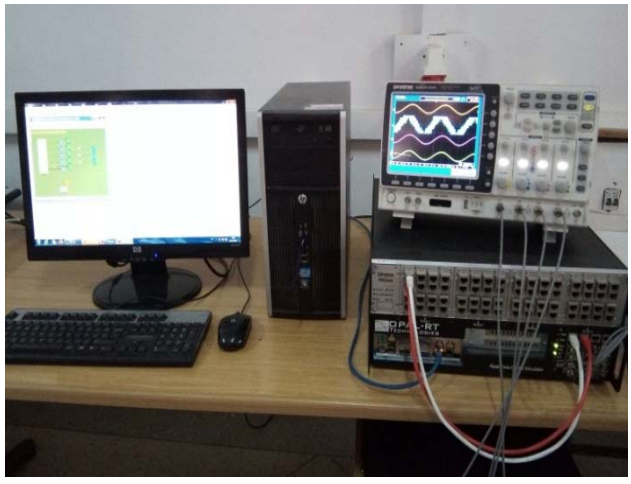

Fig. 3 – Used materials.

The studied system is simulated in using a RT-Lab Target (16 Analog inputs (OP5340), 16 Analog outputs (OP5330), 32 Digital I/O (OP5311-5312), a personal computer with MATLAB/SIMULINK/RT-Lab software and a digital oscilloscope to visualize the evolution of the different outputs.

The different parameters used in this simulation are given in Table 1.

Table 1

Parameters used in real-time simulation

Parameters	Values
E (Dc voltage)	1200 V
L (Link inductance)	0.5 mH
R (Resistance of the link inductance)	0.35 Ω
M (Mutual inductance)	0.45 mH
L_L (Load inductance)	0.8 mH
R_L (Load resistance)	0.5 Ω
f_c (Cutting frequency)	Around of 10 kHz

The obtained results are shown in Figs. 4, 5 and 6.

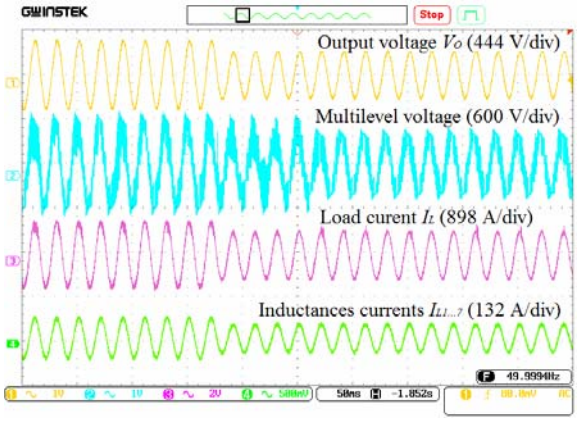

Fig. 4 – Evolution of the: 1 – output voltage V_O (444 V/div.) ; 2 – multilevel voltage (600 V/div.) ; 3 – load current I_L (898 A/div) ; 4 – inductances currents I_{L1}, I_{L2}, ..., I_{L7} (132 A/div).

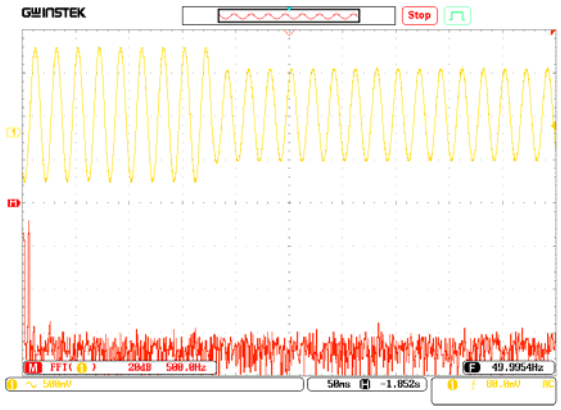

Fig. 5 – Evolution of the output voltage (V_O) with FFT.

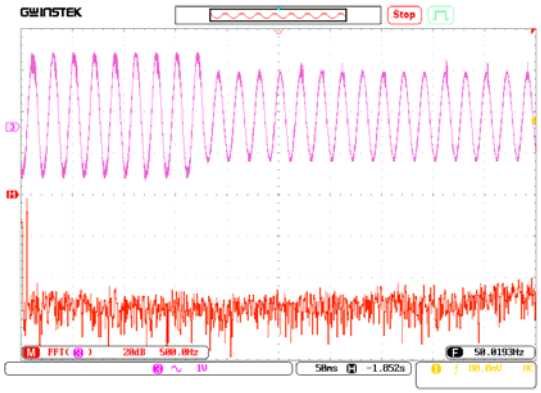

Fig. 6 – Evolution of the load current (I_L) with FFT.

The inductances current shown in Fig. 4 are stable and equilibrated. Also, we can notice that there are no ripples at their levels.

As a first variation, we decrease the reference values amplitude of inductances currents at 90 A. The response of the inductances currents is fast and instantaneous, and these currents follow this change very well. This variation causes the decrease of the load current, the output voltage and the change of the multilevel voltage form at the output of semiconductors.

A second variation is introduced (Fig. 4) where we simulate a drop in the supply voltage E of 200 V. This variation can be seen on the signal of multilevel voltage at the output of semiconductors. This disturbance does not affect the inductance currents, the load current and the output voltage.

Figures 5 and 6 show the evolution of the output voltage and the load current with their FFT analyses respectively. Both signals have a sinusoidal shape, and their THDs are 0.02 % and 0.10 %, respectively.

5. CONCLUSION

In this work a new topology of multilevel converters is presented, which is the parallel multicellular dc/ac converter including monolithic ICT. The mathematical model of this structure is given. The sliding mode control technique is proposed to control and regulate the inductances currents that are very sensitive to the variation of the input voltage of the converter.

This system is simulated in a real-time environment with RT-Lab platform. RT-Lab allows fast prototyping, minimizes the design process cost [11] and offers the possibility of modifying the parameters of the system online.

The obtained results are very satisfying, where the sliding mode control technique assures a very good regulation of the inductances currents and gives more stability to the converter. This control strategy also allows controlling the output current of the converter.

Received on September 5, 2020

REFERENCES

1. T. A. Meynard, B. Cougo, F. Forest, E. Labouré, *Parallel multicell Converters for high current: design of intercell transformers*, IEEE International Conference on Industrial Technology (ICIT), pp. 1359-1364, Vina del Mar, Chile, May, 2010.
2. P. Wong, Q. Wu, P. Xu, P. Yang, F.C. Lee, *Performance improvements of interleaving VRMs with coupling inductors*, IEEE Trans. Power Electron., **16**, *4*, pp. 499–507 (2001).
3. S. Sanchez, F. Richardeau, D. Risaletto, *Design and fault-operation analysis of a modular cyclic cascade inter-cell transformer (ICT) for parallel multicell converters*, Mathematics and Computers in Simulation, **131**, 4, pp. 190–199 (2017).
4. B. Amghar, M. Darcherif, J.P. Barbot, P. Gauthier, *Modeling and control of parallel multicell chopper using Petri nets*, 8th Power Plant and Power System Control Symposium (PPPSC'2012), Toulouse, France, 2012.
5. E. Laboure, A. Cuniere, T.A Meynard, F. Forest, E. Sarraute, *A theoretical approach to intercell transformers, application to interleaved converters*, IEEE Trans. Power Electron. **23**, *1*, pp. 464–474 (2008).
6. S. Sanchez, D. Risaletto, F. Richardeau, G. Gateau, *Comparison and design of Inter-Cell transformer structures in fault-operation for parallel multicell converters*, Energy Conversion Congress and Exposition, Pittsburgh. PA. USA, Nov. 13, 2014.
7. S. Mikkili, A. K. Panda, *Review of RT-LAB and steps involved for implementation of a Simulink model from MATLAB to REAL-TIME*, International Journal of Emerging Electric Power Systems, **14**, *6*, pp. 641–658 (2013).
8. Real time simulation [online]. Available at: https://en.wikipedia.org/wiki/Real-time_simulation.

9. M. J. Gorman, J. J. Grainger, *Transformer Modelling for Distribution System Studies. Part I: Linear Modelling Basics*, IEEE Trans. Power Delivery, **7**, *2*, pp. 567–574 (1992).
10. M. J. Gorman, J. J. Grainger, *Transformer Modelling for Distribution System Studies. Part II: Addition of Models to Y_{BUS} and Z_{BUS}*, IEEE Trans. Power Delivery, **7**, *2*, pp. 575–580 (1992).
11. S. Meradi, K. Benmansour, K. Herizi, M. Tadjine, M.S. Boucherit, *Sliding mode and fault tolerant control for multicell converter four quadrants*, Electric Power Systems Research, **95**, pp. 128–139, Feb. 2013.
12. V. Utkin, J. Guldner, J. Shi, *Sliding mode control in electromechanical systems*, Taylor & Francis, Inc., London, Philadelphia, 1999.
13. RT-LAB, Opal-RT Technologies, Inc., 1751 Richardson Suite, 2525, Montréal, Québec, H3K 1H6, Canada, 2003.
14. A. Idir, and M. Kidouche, *RT-LAB and DSPACE: Two softwares for real time control of induction motors*, Rev. Roum. Sci. Techn. – Électrotechn. et Énerg., **59**, *2*, pp. 205–214 (2014).